Measurement of Small Photon Numbers in Circuit QED Resonators

Juan Atalaya,[1,*] Alex Opremcak,[1] Ani Nersisyan,[1] Kenny Lee,[1] and Alexander N. Korotkov[1,2]
[1]Google Quantum AI, Santa Barbara, California 93111, USA
[2]Department of Electrical and Computer Engineering, University of California, Riverside, California 92521, USA

(Received 27 October 2023; accepted 9 April 2024; published 13 May 2024)

Off-resonant interaction of fluctuating photons in a resonator with a qubit increases the qubit dephasing rate. We use this effect to measure a small average number of intracavity photons that are coherently or thermally driven. For spectral resolution, we do this by subjecting the qubit to a Carr-Purcell-Meiboom-Gill sequence and record the qubit dephasing rate for various periods between qubit π pulses. The recorded data is then analyzed with formulas for the photon-induced dephasing rate derived for the non-Gaussian noise regime with an arbitrary ratio of the resonator dispersive shift to decay rate. We show that the presented Carr-Purcell-Meiboom-Gill dephasing rate formulas agree well with experimental results and demonstrate measurement of thermal and coherent photon populations at the level of a few 10^{-4}.

DOI: 10.1103/PhysRevLett.132.203601

Introduction.—In state-of-the-art circuit QED setups, dispersive interaction [1] between qubits and residual photons in readout microwave cavities has been recognized as an important source of decoherence [2–8] that can prevent T_2 times from reaching the no-pure-dephasing limit of $2T_1$ in flux [5] and transmon [8] qubits, even at the flux-insensitive point. Such residual photons can be *thermal* (due to, e.g., improperly filtered or attenuated blackbody radiation [7,8]) or *coherent* (due to, e.g., unintended driving of readout cavities), or both. To suppress but not eliminate photon-induced dephasing [2], dynamical decoupling (DD) techniques, such as the Carr-Purcell-Meiboom-Gill (CPMG) sequence [9], can be used [10]. Additionally, DD sequences have been used to probe dephasing noise spectra [11,12].

Characterization of very small intracavity photon numbers with superconducting qubits is of practical interest to the circuit QED community. Recent works have demonstrated measurement of a few 10^{-4} to a few 10^{-3} thermal photons on average [5,7,8]. This measurement capability has been used in microwave radiometry [13] and in recent improvements of microwave attenuators aimed at thermalizing microwave cavities [6,8]. Two experimental methods have been previously used to characterize average thermal or coherent intracavity photon numbers ($\bar{n}_{\rm th}$ or $\bar{n}_{\rm coh}$). The first method uses a superconducting qubit subject to Ramsey or spin-echo sequences [8,13]. An upper bound for $\bar{n}_{\rm th}$ can be inferred by assuming that measured pure dephasing rates are only due to thermal photon shot noise [14,15]. It has been reported that this method can detect thermal photon numbers of the order of a few 10^{-4} [7,8]; however, it cannot distinguish between thermal and coherent photon populations, and it can be applied to tunable qubits only at flux-insensitive points. The second method uses a spin locking protocol that probes photon shot-noise spectra [5,7]. This method can distinguish between thermal and coherent photon populations since the spectral line of the photon shot noise has a half-width of κ for thermal photons and $\kappa/2$ for coherent photons [7,16], where κ is the cavity mode decay rate. The spin locking method has been used to measure average thermal photon numbers of 6×10^{-3} and below [7].

Here, we present a method for measuring ultrasmall average photon numbers in a resonator that is based on the dephasing rate of a qubit subject to a CPMG sequence. We demonstrate this metrology technique and measure intentionally added average thermal and coherent photon numbers at the level of 5×10^{-4}. We also show that the ambient thermal photon number of our resonators is below 2×10^{-4}. In this method, the qubit's CPMG dephasing rate $\Gamma_2^{\rm cpmg}$ is measured for various periods Δt between consecutive qubit π pulses of the CPMG sequence (see Fig. 1). The specific

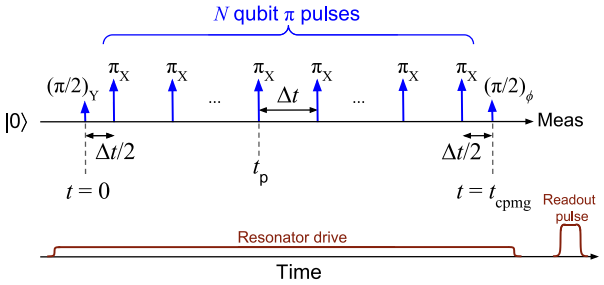

FIG. 1. Experimental procedure. The qubit is subject to a CPMG sequence with N qubit π pulses, separated by the period Δt (total duration is $t_{\rm cpmg} = N\Delta t$). At the same time, the resonator is continuously driven with a microwave tone of constant amplitude or by effectively white noise in order to add coherent or thermal photons, respectively (the resonator reaches steady state before the CPMG sequence begins at $t = 0$).

 © 2024 American Physical Society

dependence of Γ_2^{cpmg} on Δt allows us to find contributions to the qubit dephasing from thermal or coherent intracavity photons and to infer the corresponding average photon numbers $\bar{n}_{\mathrm{th}}$ and $\bar{n}_{\mathrm{coh}}$. For this purpose we derive analytical formulas for the photon-induced dephasing rate in CPMG, which are applicable for arbitrary ratios between the dispersive shift 2χ and resonator decay rate κ. Since the noise is significantly non-Gaussian when $2\chi/\kappa$ is not small, the standard filter-function approach is not applicable (as shown later). Our formulas are also useful to calculate the reduction factor of the photon-induced dephasing rate by periodic DD sequences such as CPMG and XY-4 in, e.g., quantum error correction applications [17]. The formulas show good agreement with numerical results and experimental data. Our results are also relevant to hybrid quantum systems such as vibrational modes [18] (e.g., surface [19] or bulk [20] acoustic waves) coupled to superconducting qubits or nitrogen-vacancy centers, or spin qubits dispersively coupled to microwave resonators [21].

Photon-induced dephasing in CPMG.—We consider a qubit subject to a conventional CPMG sequence that includes N π pulses, separated by a period Δt. It also includes two $\pi/2$ pulses at the beginning and end of the sequence (see Fig. 1) and has a duration $t_{\mathrm{cpmg}} = N\Delta t$. During execution of the CPMG sequence, fluctuating photons in a microwave cavity (the qubit readout resonator in our experiments) induce additional dephasing onto the qubit due to dispersive interaction Hamiltonian $H_{\mathrm{int}} = -\chi\sigma_z\hat{n}$, where $\sigma_z = |0\rangle\langle 0| - |1\rangle\langle 1|$ acts on the qubit and $\hat{n}$ is the resonator number operator.

We focus on the qubit coherence, defined as

$$\mathcal{C}(t_{\mathrm{cpmg}}) = 2|\mathrm{Tr}_{\mathrm{res}}\rho_{01}(t_{\mathrm{cpmg}})|, \tag{1}$$

where $\rho_{01} = \langle 0|\rho|1\rangle$, ρ is the qubit-resonator density matrix, and the trace is over the resonator degrees of freedom. The qubit coherence is evaluated at the moment t_{cpmg} immediately before the second $\pi/2$ pulse. Experimentally, the coherence is obtained from the qubit population difference measured after the second $\pi/2$ pulse with six equidistant values of the microwave phase ϕ, which is then fitted sinusoidally as a function of ϕ, so that $\mathcal{C}$ is the visibility (amplitude) of the oscillation. In the absence of decoherence, $\mathcal{C} = 1$. For analytics, we assume that the only source of qubit decoherence is dephasing from photon shot noise and that the qubit pulses are ideal and instantaneous.

Using the standard filter-function approach [12,22–24] based on the Gaussian approximation, for $N \gg 1$ and dephasing due to thermal photons in the resonator, we obtain exponential decay of $\mathcal{C}$ with dephasing rate

$$\Gamma_{\varphi}^{\mathrm{th,ff}} = \frac{4\chi^2\bar{n}_{\mathrm{th}}}{\kappa}\left(1 - \frac{\tanh(\kappa\Delta t/2)}{\kappa\Delta t/2}\right), \tag{2}$$

while for *resonant* coherent photons, κ in this formula should be replaced by $\kappa/2$ and the average photon number $\bar{n}_{\mathrm{th}}$ replaced by $\bar{n}_{\mathrm{coh}}$ [see Supplemental Material (SM) [25]]. These formulas assume $|2\chi| \ll \kappa$ and, as shown later, are very inaccurate (even with a prefactor) in the experimentally relevant regime of moderate or strong dispersive coupling ($|2\chi| \gtrsim \kappa$), where the qubit frequency noise cannot be approximated by a Gaussian process.

Instead of using the filter-function approach, we describe the coherence evolution $\mathcal{C}(t)$ in the way that is rigorously derived in SM [25] but can be understood physically [33] as replacing the qubit state $(|0\rangle + |1\rangle)/\sqrt{2}$ after the first $\pi/2$ pulse with either $|0\rangle$ or $|1\rangle$. Then there is no qubit-resonator entanglement, and the resonator field evolves as either $\alpha_0(t)$ or $\alpha_1(t)$, given by simple evolution equations. The coherence $\mathcal{C}$ then can be found via quantum overlap of the corresponding leaked resonator fields. The qubit coherence is [16,25,33]

$$\mathcal{C}(t_{\mathrm{cpmg}}) = \left|\left\langle \exp\left[\int_0^{t_{\mathrm{cpmg}}} \mathrm{d}t\, 2i\tilde{\chi}(t)\alpha_0(t)\alpha_1^*(t)\right]\right\rangle\right|, \tag{3}$$

where $\tilde{\chi}(t) = \pm\chi$ is a piecewise constant function that flips sign after each π pulse, and the complex-valued dynamical variables $\alpha_0(t)$ and $\alpha_1(t)$ evolve as

$$\dot{\alpha}_{0,1}(t) = -\tilde{\gamma}_{0,1}(t)\alpha_{0,1} + \sqrt{\kappa}\xi_{\mathrm{th}}(t) + \sqrt{\kappa}F_{\mathrm{d}}(t), \tag{4}$$

$$\tilde{\gamma}_q(t) = \kappa/2 - i[\delta\omega_{\mathrm{d}} + (-1)^q\tilde{\chi}(t)], \quad q = 0, 1. \tag{5}$$

Here, $F_{\mathrm{d}}(t)$ is the complex amplitude of the coherent resonator drive with frequency ω_{d} (which defines the rotating frame), $\delta\omega_{\mathrm{d}} = \omega_{\mathrm{d}} - \omega_{\mathrm{res}}$ is the detuning, and ω_{res} is the average of the resonator frequencies when the qubit is in state $|0\rangle$ or $|1\rangle$. Note that the decay factors $\tilde{\gamma}_0(t)$ and $\tilde{\gamma}_1(t)$ are complex-valued piecewise constant functions, which include detunings for the two paths of resonator evolution. Intracavity thermal population is driven by a complex-valued Gaussian white noise $\xi_{\mathrm{th}}(t)$,

$$\langle\xi_{\mathrm{th}}^*(t)\xi_{\mathrm{th}}(t')\rangle = \bar{n}_{\mathrm{th}}\delta(t - t'), \qquad \langle\xi_{\mathrm{th}}(t)\rangle = 0, \tag{6}$$

where $\bar{n}_{\mathrm{th}}$ is the average intracavity thermal photon number. The notation $\langle\cdot\rangle$ indicates averaging over noise realizations. We assume $\alpha_0(0) = \alpha_1(0) = 0$, though this is not important. If there is no coherent drive, then $F_{\mathrm{d}} = 0$ and $\delta\omega_{\mathrm{d}} = 0$. Note that Eqs. (3)–(6) are also valid for DD sequences with π pulses applied at arbitrary times [34].

We consider the experimentally relevant regime where the qubit coherence $\mathcal{C}$ decays exponentially with N (and therefore sequence duration t_{cpmg}), while still not being too small. As shown in SM [25], this occurs for CPMG sequences longer than $\sim 3\kappa^{-1}$ (or $\sim 6\kappa^{-1}$) for dephasing due to thermal (or coherent) photons, with a sufficiently small average photon number. Then evolution of $\alpha_0(t)$ and $\alpha_1(t)$ reaches a quasi-steady-state regime, in which all averages are practically periodic with period $2\Delta t$ and the

roles of $\alpha_0(t)$ and $\alpha_1(t)$ are exchanged after Δt. Only in this regime we can introduce the photon-induced qubit dephasing rate Γ_φ.

We first discuss photon-induced dephasing due to thermal photons, focusing on the limit of small average photon numbers, $\bar{n}_{\rm th} \ll 1$. In this limit, using Eq. (3), the photon-induced dephasing rate can be approximated as

$$\Gamma_\varphi^{\rm th} = -{\rm Re}\left[\int_{t_{\rm p}}^{t_{\rm p}+\Delta t} {\rm d}t\, 2i\tilde{\chi}(t)\mathcal{A}(t)\right]/\Delta t, \tag{7}$$

$$\mathcal{A}(t) \equiv \langle \alpha_0(t)\alpha_1^*(t)\rangle, \tag{8}$$

where $t_{\rm p}$ indicates the moment of one (any) of the π pulses after reaching the quasi-steady-state regime. Since in this regime α_0 and α_1 exchange their roles after Δt, we can use the approximation

$$\mathcal{A}(t+\Delta t) = \mathcal{A}^*(t). \tag{9}$$

Equation (7) assumes $\bar{n}_{\rm th} \ll 1$; a more general result is given in SM [25].

Without loss of generality, let us assume that $\tilde{\chi}(t) = \chi$ for $t \in (t_{\rm p}, t_{\rm p}+\Delta t)$. Using Eqs. (4)–(6), it is straightforward to show that $\mathcal{A}(t)$ evolves as

$$\dot{\mathcal{A}}(t) = -(\kappa - 2\chi i)\mathcal{A} + \kappa\bar{n}_{\rm th}. \tag{10}$$

Solving this equation and using the condition $\mathcal{A}(t_{\rm p}+\Delta t) = \mathcal{A}^*(t_{\rm p})$ following from Eq. (9), we find

$$\mathcal{A}(t) = e^{-\kappa_-(t-t_{\rm p})}\left[\mathcal{A}(t_{\rm p}) - \frac{\kappa\bar{n}_{\rm th}}{\kappa_-}\right] + \frac{\kappa\bar{n}_{\rm th}}{\kappa_-}, \tag{11}$$

$$\mathcal{A}(t_{\rm p}) = \frac{\kappa\bar{n}_{\rm th}}{\kappa_-} - i\kappa\bar{n}_{\rm th}\frac{{\rm Im}[\kappa_-^{-1}](1-e^{-\kappa_-\Delta t})^*}{\sinh(\kappa\Delta t)e^{-\kappa\Delta t}}, \tag{12}$$

where $\kappa_- \equiv \kappa - 2\chi i$. Using this solution for $\mathcal{A}(t)$, we evaluate the integral in Eq. (7) with $\tilde{\chi}(t) = \chi$ and obtain the thermal-photon-induced dephasing rate ($\bar{n}_{\rm th} \ll 1$),

$$\Gamma_\varphi^{\rm th}(\Delta t, \bar{n}_{\rm th}) = \frac{4\chi^2\bar{n}_{\rm th}}{\kappa[1+(2\chi/\kappa)^2]}\mathcal{R}_{\rm th}(\Delta t), \tag{13}$$

$$\mathcal{R}_{\rm th}(\Delta t) = 1 - \frac{\cosh(\kappa\Delta t) - \cos(2\chi\Delta t)}{(\kappa\Delta t/2)[1+(2\chi/\kappa)^2]\sinh(\kappa\Delta t)}, \tag{14}$$

where the first term in Eq. (13) is the low-frequency limit ($\Delta t \to \infty$) of the qubit dephasing rate, which agrees with Eqs. (11),(12) of Ref. [14] and Eq. (44) of Ref. [15], while $\mathcal{R}_{\rm th}$ is the reduction factor ($0 \le \mathcal{R}_{\rm th} \le 1$) due to the CPMG sequence with interpulse period Δt (note that $\mathcal{R}_{\rm th} \to 1$ as $\Delta t \to \infty$ and $\mathcal{R}_{\rm th} \to 0$ as $\Delta t \to 0$). Equations (13) and (14) are our main result for the dephasing rate from thermal photons; it reduces to Eq. (2) when $2\chi/\kappa \ll 1$.

We now discuss dephasing due to coherent photons, using Eqs. (3)–(5) without the noise term, $\xi_{\rm th} = 0$, and without averaging in Eq. (3). We assume a constant coherent drive amplitude, $F_{\rm d}(t) = F_{\rm d}^{\rm dc}$.

In the regime of exponential decay of the coherence, the photon-induced dephasing rate $\Gamma_\varphi^{\rm coh}$ from coherent photons can still be obtained from Eq. (7), in which $\mathcal{A}(t) = \alpha_0(t)\alpha_1^*(t)$ no longer requires averaging, but the time interval $(t_{\rm p}, t_{\rm p}+\Delta t)$ should still assume reaching the quasi-steady-state regime, for which we can use approximation

$$\alpha_0(t+\Delta t) = \alpha_1(t), \qquad \alpha_1(t+\Delta t) = \alpha_0(t). \tag{15}$$

Note that for coherent driving $\bar{n}_{\rm coh}$ is not necessarily small, as long as the resulting dephasing rate is sufficiently small: $\Gamma_\varphi^{\rm coh} \ll \min(1/\Delta t, \kappa)$.

Proceeding as in the case of thermal photons, we solve Eq. (4) to obtain the trajectories $\alpha_0(t)$ and $\alpha_1(t)$ within the time interval $(t_{\rm p}, t_{\rm p}+\Delta t)$ and use the condition Eq. (15) with $t = t_{\rm p}$ to find the initial values. Substituting the result into Eq. (7) and calculating the integral, we obtain the dephasing rate $\Gamma_\varphi^{\rm coh}$ due to fluctuating coherent photons in the resonator. In the case of no detuning, $\delta\omega_{\rm d} = 0$, the final result is

$$\Gamma_\varphi^{\rm coh}(\Delta t, \bar{n}_{\rm coh}) = \frac{8\chi^2\bar{n}_{\rm coh}}{\kappa[1+(2\chi/\kappa)^2]}\mathcal{R}_{\rm coh}(\Delta t), \tag{16}$$

$$\mathcal{R}_{\rm coh}(\Delta t) = 1 - \frac{\cosh(\kappa\Delta t/2) - \cos(\chi\Delta t)}{(\kappa\Delta t/4)\sinh(\kappa\Delta t/2)[1+(2\chi/\kappa)^2]} \times \left[1 + \frac{\chi}{\kappa}\frac{\sin(\chi\Delta t)}{\sinh(\kappa\Delta t/2)} - 2\left(\frac{\chi}{\kappa}\right)^2\right], \tag{17}$$

where $\bar{n}_{\rm coh} = \kappa|F_{\rm d}^{\rm dc}|^2/[(\kappa/2)^2+\chi^2]$ is the average intracavity photon number for both qubit states $|0\rangle$ and $|1\rangle$ (without CPMG), while the factor $\mathcal{R}_{\rm coh}(\Delta t)$ is due to the CPMG sequence with period Δt. In the limit $\Delta t \to \infty$, we get $\mathcal{R}_{\rm coh} \to 1$ and our result for $\Gamma_\varphi^{\rm coh}$ agrees with the dephasing rate given by Eq. (69) of Ref. [15], Eq. (5.20) of Ref. [16], and Eq. (17) of Ref. [35]. When $\Delta t \to 0$, we get $\mathcal{R}_{\rm coh} \to 0$. Note that $\mathcal{R}_{\rm coh}$ can exceed 1 when $2\chi/\kappa > 1.393$ and $(2\chi/2\pi)\Delta t$ is near an odd integer. It is easy to check that the result Eq. (16) approaches the filter-function result [Eq. (2) with $\kappa \to \kappa/2$] when $2\chi/\kappa \ll 1$. In the case of a nonzero detuning $\delta\omega_{\rm d}$, the formula for $\Gamma_\varphi^{\rm coh}(\Delta t, \bar{n}_{\rm coh})$ is given in SM [25].

While the analytical results (13), (14) and (16), (17) assume instantaneous π pulses, they agree well (somewhat surprisingly) with numerical simulations even when pulse duration occupies up to half of Δt and is comparable to $1/\kappa$ [25]. We emphasize that the results for $\Gamma_\varphi^{\rm coh}$ and $\Gamma_\varphi^{\rm th}$ hold for

an arbitrary ratio $2\chi/\kappa$, in contrast to the filter-function result, Eq. (2), which is valid only if $2\chi/\kappa \ll 1$.

Experimental results.—To benchmark our formulas and to measure photon-induced dephasing rate due to thermal and coherent photons in a resonator with metrological precision, we perform experiments using the procedure depicted in Fig. 1. Our experiments are conducted in the moderate dispersive coupling regime with a ratio $2\chi/\kappa \approx 0.7$, where $\kappa = (19.4\ \text{ns})^{-1} = 2\pi \times 8.2$ MHz and $2\chi = 2\pi \times 5.7$ MHz. The qubit pulses have a duration of 25 ns, which limits the minimum period Δt of π pulses (we use $\Delta t \geq 40$ ns, so that the CPMG sequence frequency $f_s \equiv 1/2\Delta t$ is limited to 12.5 MHz). We use a tunable 2D transmon with frequency $\omega_q = 2\pi \times 4.1$ GHz (nonlinearity is $\eta = 229$ MHz and $T_1 \simeq 60$ μs), set near the flux-insensitive point, and a resonator with frequency $\omega_{\text{res}} = 2\pi \times 5.2$ GHz. Fabrication, qubit control and readout are similar to that of the Sycamore processor [17,36]. An important feature of our metrology method is its simpler calibration and implementation compared to the spin locking [5,7].

We first discuss experimental results for qubit dephasing from thermal photons. Ambient thermal population in the resonator is too small for a confident fit with our formula. Therefore, we controllably add thermal photons to the resonator by driving it with an engineered broadband noise as in Refs. [3,5,7,8]. The correlation time of the applied noise is roughly 1 ns, much shorter than the resonator decay time κ^{-1}, which sets the correlation time of the thermal photon number fluctuations inside the resonator. By varying the applied noise power $\mathcal{P}_{\text{drive}}$, we vary the total average photon number, $\bar{n}_{\text{th}} = \bar{n}_{\text{th}}^{\text{add}} + \bar{n}_{\text{th}}^{\text{amb}}$, where $\bar{n}_{\text{th}}^{\text{amb}}$ denotes the ambient thermal photon population in the resonator and $\bar{n}_{\text{th}}^{\text{add}} \propto \mathcal{P}_{\text{drive}}$ denotes the added photon number. The proportionality coefficient between $\bar{n}_{\text{th}}^{\text{add}}$ and $\mathcal{P}_{\text{drive}}$ is calibrated by using spin-echo dephasing data, as discussed in SM [25].

The CPMG dephasing rates Γ_2^{cpmg} are obtained from measurements of the qubit coherence $\mathcal{C}$, fixing Δt and changing N in the CPMG sequence. The number N of qubit π pulses is chosen to be $N \geq 2$ and we check that $\kappa N \Delta t \geq 4$ to avoid the initial nonexponential decay regime of the qubit coherence (ideally $N \gg 1$ and $\kappa N \Delta t \gg 1$); the chosen N are even and correspond to $N\Delta t$ separation by about 1 μs. We find that $\mathcal{C}$ decays exponentially with the sequence duration (see Fig. S3 in SM [25]), and then an exponential fit yields the sought Γ_2^{cpmg} for a given Δt. For our method, it is important to have good exponential fits; see dashed lines in Figs. S3 and S4 in SM [25].

Figure 2 shows the measured dephasing rate Γ_2^{cpmg} as a function of the CPMG sequence frequency $f_s = 1/2\Delta t$ (in the filter-function approach, the noise at f_s gives the main contribution to Γ_2^{cpmg} [25]) for added thermal photon populations $\bar{n}_{\text{th}}^{\text{add}} = 0$ (blue), 5×10^{-4} (orange) and 10^{-3} (green). The experimental data is indicated by symbols and

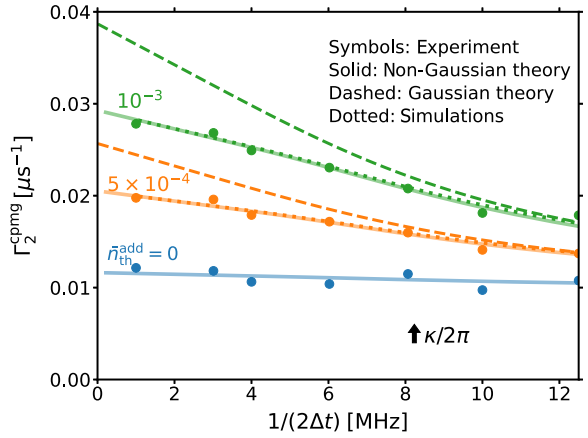

FIG. 2. CPMG dephasing rate in the presence of thermal photons. The CPMG dephasing rates as functions of the CPMG sequence frequency $f_s = 1/2\Delta t$ are shown for added thermal populations of $\bar{n}_{\text{th}}^{\text{add}} = 0$ (blue), 5×10^{-4} (orange), and 10^{-3} (green). Symbols indicate the experimental data and solid lines are fits based on Eqs. (13) and (14) with a pedestal $\Delta\Gamma_2$. The dashed lines show the filter-function theory [Eq. (2)] and the dotted lines show numerical results that include the shape and duration (25 ns) of the experimental qubit pulses.

the solid lines show the theoretical fit for the CPMG dephasing rate,

$$\Gamma_2^{\text{cpmg}} = \Gamma_\varphi^{\text{th}}(\Delta t, \bar{n}_{\text{th}}) + \Delta\Gamma_2, \tag{18}$$

where $\Gamma_\varphi^{\text{th}}$ is given by Eqs. (13) and (14) and $\Delta\Gamma_2$ is the dephasing rate contribution not related to photon shot noise, assumed to be independent of Δt. We fit all experimental data points of Fig. 2 using four fitting parameters: three values of $\bar{n}_{\text{th}}$ and common $\Delta\Gamma_2$. Then we obtain $\Delta\Gamma_2 = (101.0\ \mu\text{s})^{-1}$ and the photon populations $\bar{n}_{\text{th}} = (1.0 \pm 0.4) \times 10^{-4}$, $(6.3 \pm 0.4) \times 10^{-4}$, and $(1.15 \pm 0.04) \times 10^{-3}$ for the blue, orange, and green lines, respectively. These values of $\bar{n}_{\text{th}}$ are consistent with intended values of $\bar{n}_{\text{th}}^{\text{add}}$ and additional contribution from ambient population $\bar{n}_{\text{th}}^{\text{amb}}$ of crudely 1.3×10^{-4}. If we fit only the blue points ($\bar{n}_{\text{th}}^{\text{add}} = 0$), we get $\bar{n}_{\text{th}}^{\text{amb}} = (1.5 \pm 0.8) \times 10^{-4}$ and $\Delta\Gamma_2 = (106.9\ \mu\text{s})^{-1}$. From these results we conclude that the ambient thermal photon number is below 2×10^{-4} and the inaccuracy of our method for $\bar{n}_{\text{th}}^{\text{amb}}$ is crudely 10^{-4}.

We emphasize a very good agreement in Fig. 2 between the experimental data and our analytical theory (orange and green solid lines). This is in sharp contrast with the Gaussian-approximation-based filter-function theory, Eq. (2), depicted by the dashed lines, for which we use the same values of $\bar{n}_{\text{th}}$ and $\Delta\Gamma_2$ that were obtained from the above fits. If in Eq. (2) we replace $\bar{n}_{\text{th}}$ with $\bar{n}_{\text{th}}/[1 + (2\chi/\kappa)^2]$ to get agreement with Eq. (13) in the low-frequency case, $1/(2\Delta t) \to 0$, then there will be a significant disagreement for $1/(2\Delta t)$ comparable or bigger than κ. The dotted lines in Fig. 2 show numerical results, which

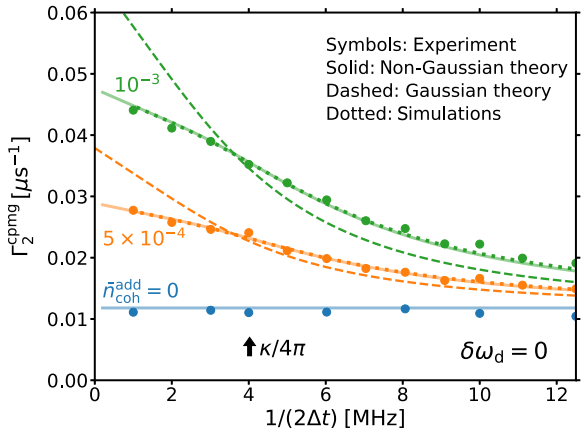

FIG. 3. CPMG dephasing rate in the presence of coherent photons. The experimental data (symbols) correspond to added coherent photon populations of $\bar{n}_{\rm coh}^{\rm add} = 0$ (blue), 5×10^{-4} (orange), and 10^{-3} (green). Solid lines depict our theory prediction while the dashed lines indicate the filter-function theory prediction. The dotted lines depict numerical results that include the shape and duration of experimental π pulses.

take into account the shape and duration of the π pulses. We see that these lines practically coincide with the solid lines, so our analytics works very well, only slightly underestimating the dephasing rate for short Δt comparable with the pulse duration.

The symbols in Fig. 3 show the measured CPMG dephasing rates $\Gamma_2^{\rm cpmg}$ for various interpulse periods Δt (converted to frequency $1/2\Delta t$) for added coherent photon populations $\bar{n}_{\rm coh}^{\rm add} = 0$ (blue), 5×10^{-4} (orange) and 10^{-3} (green) due to applied on-resonance drive, $\delta\omega_{\rm d} = 0$. Note that blue symbols are different from those in Fig. 2 (a different experiment a few hours apart). We now fit the experimental data in Fig. 3 as $\Gamma_\varphi^{\rm coh}(\Delta t, \bar{n}_{\rm coh}) + \Delta\Gamma_2$ (solid lines), where $\Gamma_\varphi^{\rm coh}$ is given by Eqs. (16) and (17) and we have neglected contributions due to thermal photons. Using four fitting parameters (three values of $\bar{n}_{\rm coh}$ and a common $\Delta\Gamma_2$), we obtain $\bar{n}_{\rm coh} = 2 \times 10^{-8}$, 4.9×10^{-4}, and 1.03×10^{-3}, which are very close to the intended values of $\bar{n}_{\rm coh}^{\rm add}$, and $\Delta\Gamma_2 = (84.8\ \mu{\rm s})^{-1}$. The difference in $\Delta\Gamma_2$ compared with fitting data in Fig. 2 is due to $\bar{n}_{\rm th}^{\rm amb}$. Note that if in Fig. 3 we include $\bar{n}_{\rm th}^{\rm amb}$ as the fifth fitting parameter, we obtain $\bar{n}_{\rm th}^{\rm amb} \simeq 10^{-10}$, while if we fit only the blue symbols (with $\bar{n}_{\rm coh} = 0$), we obtain $\bar{n}_{\rm th}^{\rm amb} = (0.5 \pm 0.4) \times 10^{-4}$. These results are consistent with the method inaccuracy of about 10^{-4}.

In Fig. 3 we again see very good agreement between experiment and our analytical theory (orange and green solid lines), which is in sharp contrast to the filter-function theory shown by the dashed lines (using the same $\bar{n}_{\rm coh}$ and $\Delta\Gamma_2$). The dotted lines depict numerical results where we include the shape and duration (25 ns) of the experimental qubit pulses; numerics practically coincide with analytics.

Conclusions.—We have derived and validated formulas for the CPMG dephasing rate of a qubit due to thermal and coherent photons inside a resonator. These formulas are valid for an arbitrary ratio $2\chi/\kappa$, accounting for non-Gaussian noise. We have also demonstrated that these formulas and CPMG data can be used to measure average thermal and coherent intracavity photon populations at the level of $\sim 10^{-4}$ photons. This level of accuracy is probably limited by fluctuations of the qubit T_1 and other parameters.

We thank the Google Quantum AI team for fabrication of the measured device and for building and maintaining the hardware and software infrastructure used in this work. We also thank Mark I. Dykman for a significant contribution during the early stage of this work and for useful discussions.

*Corresponding author: jatalaya@google.com

[1] A. Blais, A. L. Grimsmo, S. M. Girvin, and A. Wallraff, Rev. Mod. Phys. **93**, 025005 (2021).
[2] P. Bertet, I. Chiorescu, G. Burkard, K. Semba, C. J. P. M. Harmans, D. P. DiVincenzo, and J. E. Mooij, Phys. Rev. Lett. **95**, 257002 (2005).
[3] A. P. Sears, A. Petrenko, G. Catelani, L. Sun, H. Paik, G. Kirchmair, L. Frunzio, L. I. Glazman, S. M. Girvin, and R. J. Schoelkopf, Phys. Rev. B **86**, 180504(R) (2012).
[4] C. Rigetti, J. M. Gambetta, S. Poletto, B. L. T. Plourde, J. M. Chow, A. D. Córcoles, J. A. Smolin, S. T. Merkel, J. R. Rozen, G. A. Keefe, M. B. Rothwell, M. B. Ketchen, and M. Steffen, Phys. Rev. B **86**, 100506(R) (2012).
[5] F. Yan, S. Gustavsson, A. Kamal, J. Birenbaum, A. P. Sears, D. Hover, T. J. Gudmundsen, D. Rosenberg, G. Samach, S. Weberand, J. L. Yoder, T. P. Orlando, J. Clarke, A. J. Kerman, and W. D. Oliver, Nat. Commun. **7**, 12964 (2016).
[6] J.-H. Yeh, J. LeFebvre, S. Premaratne, F. C. Wellstood, and B. S. Palmer, J. Appl. Phys. **121**, 224501 (2017).
[7] F. Yan, D. Campbell, P. Krantz, M. Kjaergaard, D. Kim, J. L. Yoder, D. Hover, A. Sears, A. J. Kerman, T. P. Orlando, S. Gustavsson, and W. D. Oliver, Phys. Rev. Lett. **120**, 260504 (2018).
[8] Z. Wang, S. Shankar, Z. K. Minev, P. Campagne-Ibarcq, A. Narla, and M. H. Devoret, Phys. Rev. Appl. **11**, 014031 (2019).
[9] S. Meiboom and D. Gill, Rev. Sci. Instrum. **29**, 688 (1958).
[10] Google Quantum AI, Nature (London) **595**, 383 (2021).
[11] J. Bylander, S. Gustavsson, F. Yan, F. Yoshihara, K. Harrabi, G. Fitch, D. G. Cory, Y. Nakamura, J.-S. Tsai, and W. D. Oliver, Nat. Phys. **7**, 565 (2011).
[12] C. L. Degen, F. Reinhard, and P. Cappellaro, Rev. Mod. Phys. **89**, 035002 (2017).
[13] Z. Wang, M. Xu, X. Han, W. Fu, S. Puri, S. M. Girvin, H. X. Tang, S. Shankar, and M. H. Devoret, Phys. Rev. Lett. **126**, 180501 (2021).
[14] M. I. Dykman and M. A. Krivoglaz, Sov. Phys. Solid State **29**, 210 (1987).

[15] A. A. Clerk and D. W. Utami, Phys. Rev. A **75**, 042302 (2007).
[16] J. Gambetta, A. Blais, D. I. Schuster, A. Wallraff, L. Frunzio, J. Majer, M. H. Devoret, S. M. Girvin, and R. J. Schoelkopf, Phys. Rev. A **74**, 042318 (2006).
[17] Google Quantum AI, Nature (London) **614**, 676 (2023).
[18] A. Bachtold, J. Moser, and M. I. Dykman, Rev. Mod. Phys. **94**, 045005 (2022).
[19] K. J. Satzinger *et al.*, Nature (London) **563**, 661 (2018).
[20] Y. Chu, P. Kharel, W. H. Renninger, L. D. Burkhart, L. Frunzio, P. T. Rakich, and R. J. Schoelkopf, Science **358**, 199 (2017).
[21] G. Burkard, T. D. Ladd, A. Pan, J. M. Nichol, and J. R. Petta, Rev. Mod. Phys. **95**, 025003 (2023).
[22] L. Cywiński, R. M. Lutchyn, C. P. Nave, and S. Das Sarma, Phys. Rev. B **77**, 174509 (2008).
[23] T. Yuge, S. Sasaki, and Y. Hirayama, Phys. Rev. Lett. **107**, 170504 (2011).
[24] G. A. Álvarez and D. Suter, Phys. Rev. Lett. **107**, 230501 (2011).
[25] See Supplemental Material at http://link.aps.org/supplemental/10.1103/PhysRevLett.132.203601 for derivation of Eq. (3), CPMG dephasing rate formulas for finite frequency detuning $\delta\omega_d$, numerical results for CPMG dephasing rate with π pulses of finite duration, and filter-function approach, which includes Refs. [26–32].
[26] C. W. Gardiner and P. Zoller, *Quantum Noise*, 3rd ed. (Springer, Berlin, 2004).
[27] J. Gambetta, A. Blais, D. I. Schuster, A. Wallraff, L. Frunzio, J. Majer, M. H. Devoret, S. M. Girvin, and R. J. Schoelkopf, Phys. Rev. A **74**, 042318 (2006).
[28] J. Atalaya, M. Khezri, and A. N. Korotkov, Phys. Rev. A **99**, 043810 (2019).
[29] A. Blais, R.-S. Huang, A. Wallraff, S. M. Girvin, and R. J. Schoelkopf, Phys. Rev. A **69**, 062320 (2004).
[30] P. Krantz, M. Kjaergaard, F. Yan, T. P. Orlando, S. Gustavsson, and W. D. Oliver, Appl. Phys. Rev. **6**, 021318 (2019).
[31] T. Green, H. Uys, and M. J. Biercuk, Phys. Rev. Lett. **109**, 020501 (2012).
[32] A. A. Clerk, M. H. Devoret, S. M. Girvin, F. Marquardt, and R. J. Schoelkopf, Rev. Mod. Phys. **82**, 1155 (2010).
[33] A. N. Korotkov, Phys. Rev. A **94**, 042326 (2016).
[34] G. S. Uhrig, Phys. Rev. Lett. **98**, 100504 (2007).
[35] M. Khezri, J. Dressel, and A. N. Korotkov, Phys. Rev. A **92**, 052306 (2015).
[36] F. Arute *et al.*, Nature (London) **574**, 505 (2019).